Low-Complexity Smart Antenna Methods for Third-Generation W-CDMA Systems

George V. Tsoulos, *Member, IEEE*, Georgia E. Athanasiadou, *Member IEEE*, and Robert J. Piechocki, *Student Member IEEE*

***Abstract*—There is still an open debate within the research community regarding the likely performance enhancement of smart antennas versus their complexity for commercial wireless applications. The goal of the study presented in this paper is to investigate the performance improvement attainable using relatively simple smart antenna techniques when applied to the third-generation W-CDMA air interface. Methods to achieve this goal include fixed multibeam architectures with different beam selection algorithms (maximum power criterion, combined beams) or adaptive solutions driven by relatively simple direction finding algorithms. After comparing these methods against each other for several representative scenarios, some issues related to the sensitivity of these methods are also studied, (e.g., robustness to environment, mismatches originating from implementation limitations, etc.). Results indicate that overall, conventional beamforming seems to be the best choice in terms of balancing the performance and complexity requirements, in particular when the problem with interfering high-bit-rate W-CDMA users is considered.**

***Index Terms*—Adaptive algorithms, smart antennas, third generation systems, wavelength code division mupltiple access (WCDMA).**

I. Introduction

OVER the last few years, the demand for service provision via the wireless communication bearer has risen beyond all expectations. If this extraordinary capacity demand is put in the context of third-generation systems requirements (UMTS, IMT2000) [1], then the most demanding technological challenge emerges: the need to increase the spectrum efficiency of wireless networks. While great effort in second-generation wireless communication systems has focused on the development of modulation, coding, protocols, etc., the antenna-related technology has received significantly less attention up to now. In order to achieve the ambitious requirements introduced for future wireless systems, new "intelligent" or "self-configured" and highly efficient systems, will be most certainly required. In the pursuit for schemes that will solve these problems, attention has turned into spatial filtering methods using advanced antenna techniques: adaptive or smart antennas. Filtering in the space domain can separate spectrally and temporally overlapping signals from multiple mobile units, and hence the performance of a system can be significantly improved. In this context, the operational benefits that can be achieved with exploitation of smart antenna techniques can be summarized as follows [2]:

1) more efficient power control;
2) smart handover;
3) support of value-added services:
   a) better signal quality;
   b) higher data rates;
   c) user location for emergency calls;
   d) location of fraud perpetrators;
   e) location sensitive billing;
   f) on-demand location specific services;
   g) vehicle and fleet management;
4) smart system planning;
5) coverage extension;
6) reduced transmit power;
7) smart link budget balancing;
8) increased capacity.

Much research has been performed over the last few years on adaptive methods that can achieve the above benefits, e.g., [3]–[17]. Nevertheless, it has been recognized that communication systems will exploit different advantages or mixtures of advantages offered by smart antennas, depending on the maturity of the underlying system. For example, at the beginning, costs can be reduced by exploiting the range extension capabilities of simple and cheap smart antennas. Then costs can be further decreased by avoiding extensive use of small cells where there is increased capacity demand, by exploiting the capability of smart antennas to increase capacity, with relatively simple (more complex than the previous phase) adaptive methods. Finally, more advanced systems (third generation) will be able to benefit from smart antenna systems, but it is almost certain that more sophisticated space/time filtering approaches (e.g., [17]) will be necessary to achieve the goals of universal mobile telecommunications service (UMTS), especially as these systems become mature too.

Recognizing that full exploitation of smart antennas, and in particular in future-generation systems, requires the growth of radio-frequency and digital signal-processing technology, this paper focuses on studying the performance of a UMTS-type system [wireless code-division multiple access (W-CDMA)], with relatively simple (in terms of complexity), smart antenna methods. The next section will describe the simulation method that was employed in order to achieve this goal. Then simulation results will be presented and discussed in the context of the achieved performance under different conditions.

Manuscript received September 17, 1999; revised April 6, 2000. This work was carried out at he University of Bristol, and was supported by the CEC under European collaborative project SUNBEAM (Smart Universal BEAMforming).

G. Tsoulos is with the Cambridge Technology Centre, PA Consulting Group, Hertfordshire SG8 6DP U.K. (e-mail: gtsoulos@hotmail.com)

G. Athanasiadou is with Adaptive Broadband Ltd., Cambridge CB4 1YG U.K. (e-mail: gathanasiadou@hotmail.com)

R. Piechocki is with the University of Bristol, Bristol BS8 1UB U.K.

Publisher Item Identifier S 0018-9545(00)09171-4.

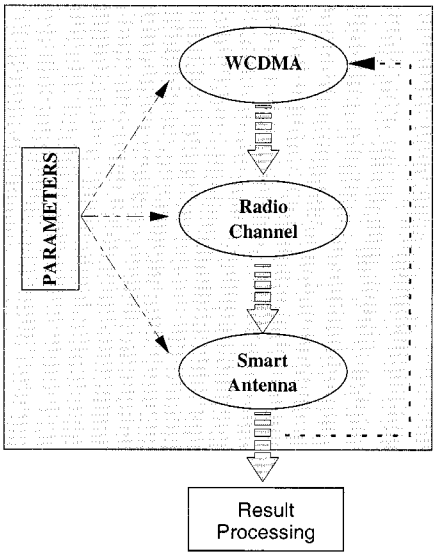

Fig. 1. Simulation concept.

II. Description of the Different Simulation Blocks

Fig. 1 outlines the concept of the simulator that was developed to perform the analysis described above. Four different blocks can be recognized from Fig. 1: 1) the W-CDMA, 2) the radio channel, 3) the smart antenna, and 4) the result processing.

A. The W-CDMA System

1) General Description: The universal mobile telecommunications system (UMTS UTRA) FRAMES mode-2 W-CDMA proposal (FMA2) [18] is based on W-CDMA, with all the users sharing the same carrier under the direct-sequence CDMA (DS-CDMA) principle. The studies shown in this paper consider only the frequency-division duplexing (FDD) mode; however, a time-division duplexing (TDD) mode for W-CDMA is also included in the specification. The FMA2 is asynchronous with no base-station dependence upon external timing source (e.g., global positioning system). It employs 10-ms frame length, which, although it is different from the global system for mobile communications (GSM), also allows making intersystem handoffs, since 12 FMA2 frames are equal to a single GSM multiframe of length 120 ms.

FMA defines two types of dedicated physical channels on both uplink and downlink: the dedicated physical control channel (PCCH) and the dedicated physical data channel (PDCH). The PCCH is needed to transmit pilot symbols for coherent reception, power-control signaling bits, and rate information for rate detection. Table I includes some of the key parameters of the discussed W-CDMA system.

The FMA2 downlink is similar to second-generation DS-CDMA systems like IS-95. The PDCH and PCCH are time multiplexed within each frame and fed to the serial-to-parallel converter. Then, both I and Q branches are spread by the same channelization orthogonal variable spreading factor (OVSF) codes and subsequently scrambled by a cell-specific code. The downlink scrambling code is a 40 960 chip segment (one frame) of a Gold code of length $2^{18}-1$. The channelization codes are OVSF codes that preserve orthogonality between channels

TABLE I
Parameters of the W-CDMA System

Multiple access method	DS-CDMA
Duplexing method	Frequency division duplex FDD
Base station synchronisation	Asynchronous operation
Chip rate	4.096 Mcps (expandable to 8.192 Mcps and 16.384 Mcps)
Frame length	10 ms
Multirate concept	Variable spreading factor and multicode Rate matching with repetition coding or puncturing Continuous transmission Rate changes dynamically frame-by-frame
Rate detection	Rate information in each frame protected with a block code and/or blind rate detection
Interleaving	Inter-frame / Intra-frame
Spreading factor	4 to 256
Spreading codes	UL: Short codes VL Kasami 256, long code optional DL: Short code, orthogonal extended Gold 256
Modulation	UL: Dual channel QPSK with complex scrambling DL: Dual channel QPSK
Pulse shaping	Root raised cosine, roll off = 0.22
Intra-frequency handover	Mobile controlled soft handover
Inter-frequency handover	Dual receiver slotted mode
Detection	UL: Coherent detection (reference symbol based) DL: Coherent detection (pilot code or reference symbol based)
Power control	UL: Open loop and fast closed loop DL: Fast closed loop
Diversity	Multipath diversity with RAKE, Antenna diversity in up-link
Adaptive Antenna support	Connection dedicated pilot bits on UL and DL

with different rates and spreading factors. Each level of the tree corresponds to a different spreading factor. A code from the tree can be used if and only if no other codes are used from an underlying branch or the path to the root of the tree. All codes form the tree cannot be used simultaneously if orthogonality is to be preserved. In essence, codes generated with this method are Walsh–Hadammard codes, with small differences in the permuting rows of each level, in order to preserve interlevel orthogonality.

Two basic options for multiplexing physical control channels are: time multiplexing and code multiplexing. In FMA2, a combined IQ and code-multiplexing solution (dual-channel quaternary phase-shift keying) is used to avoid audible interference problems with discontinuous transmission. This solution also provides robust rate detection since rate information is transmitted with fixed spreading factor on the PCCH.

In terms of the uplink spreading and scrambling concepts of the PDCH and PCCH physical channels, the physical channels are mapped onto I and Q branches, respectively, and then both branches are spread by two different OVSF channelization codes and scrambled by the complex code. Each part of the complex scrambling code is a short Kasami code—256 chips long. As a second option, long-code complex scrambling may also be used. Such a long code is an advantage for the conventional receiving scheme (single-user matched filtering), since it prevents consecutive realization of bad multiple-access interference (MAI). However, it is a disadvantage from the point of view of implementing multiuser detection, since the detector must be time-varying and explicit knowledge of interference is required.

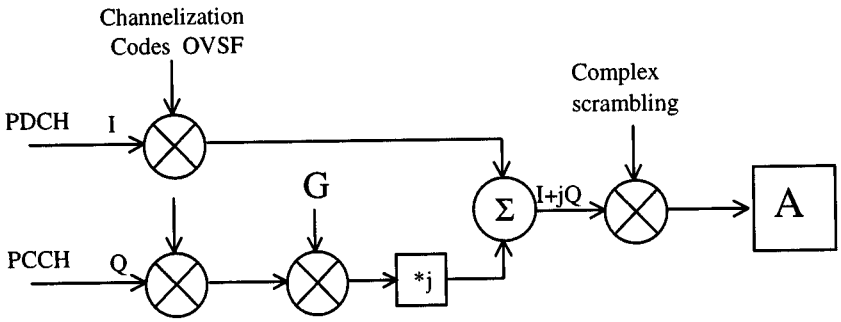

Fig. 2. Desired user simulation schematic.

2) Simulating the UTRA FDD W-CDMA System[19]: The studies performed in this paper only consider the case of a single desired user scenario with spatial combining followed by conventional matched filtering. The simulations were performed at chip level, and the following assumptions were made.

1) Perfect power control.
2) Perfect channel estimation.
3) One chip is represented by one sample—hence no pulse-shaping.
4) All users [including low bit rate (LBR)] are modeled according to the W-CDMA UTRA frame format, and also spreading/despreading and scrambling/descrambling are incorporated in the simulator. This is done to take into account site-specific radio channel models (ray tracing) where even LBR interfering users color the spatial structure of MAI.
5) Interfering users from other than the central cells are modeled as space–time white noise. Fig. 2 depicts the simulation schematic of the desired user. Since the data from other users are of no interest (single-user detection), the interfering users from the same cell are further simplified.

Same-cell interferers are constructed to account for MAI only; hence only scrambling codes are transmitted (see Fig. 3). This can be viewed also as a stream of "1" spread by the first OVSF code. Fig. 4 depicts one way to visualize or model the transmission of such signals through the radio channel with the help of a bank of tapped delay lines. The values of the parameters shown in Fig. 4 are taken from the results produced with the help of the ray-tracing propagation model described in the next section.

The reception process discussed above can be described as

$$\boldsymbol{x}(t)=\sum_{k=1}^{K}\sum_{l=1}^{L}\sqrt{p_{k,l}}s(t-\tau_{k,l})g_{k,l}(t-\tau_{k,l})\boldsymbol{a}_{k,l}+\boldsymbol{n}(t) \quad (1)$$

where $\boldsymbol{x}$ is the received signal vector by the N element antenna array, K is the number of users, L is the number of multipaths, $p_{k,l}$ is the power of the lth multipath component from the kth user, g is the scrambling code, $\boldsymbol{a}$ is the antenna response vector, $\boldsymbol{n}$ is the noise vector, and s is

$$\begin{aligned}s(t-\tau_{k,l})=&c_{k,l}^{\mathrm{PDCH}}(t-\tau_{k,l})\,b_{k,l}^{\mathrm{PDCH}}(t-\tau_{k,l})\\&+j\cdot c_{k,l}^{\mathrm{PCCH}}(t-\tau_{k,l})\,b_{k,l}^{\mathrm{PCCH}}(t-\tau_{k,l}) \quad (2)\end{aligned}$$

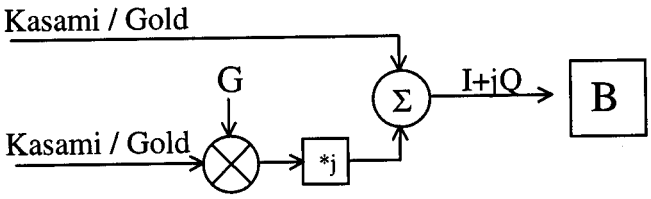

Fig. 3. Same-cell interfering users simulation schematic.

with c^{PDCH} the OVSF code assigned to the data channel (PDCH), b^{PDCH} the data bits, c^{PCCH} the OVSF code assigned to the control channel (PCCH), and b^{PCCH} the control bit sequence.

The received despread PCCH signal can be expressed as

$$\boldsymbol{y}(t)=-j\cdot\int_{\tau}^{T+\tau}g_{k,l}(t-\tau_{k,l})c_{k,l}^{\mathrm{PCCH}}(t-\tau_{k,l})\boldsymbol{x}(t)\,dt. \quad (3)$$

Finally, the despread sampled (N_s samples) correlation matrix is

$$\boldsymbol{R}_{\boldsymbol{xx}}=\frac{1}{N_s}\sum_{i=1}^{N_S}\boldsymbol{y}(t)\boldsymbol{y}^{H}(t). \quad (4)$$

B. The Radio Channel Model

Due to the site-specific nature of the spatial information needed for simulations with smart antennas, a three-dimensional (3-D) image-based ray-tracing model for small- to medium-sized cells developed at the University of Bristol [20] was employed here. Ray-tracing techniques have emerged as a dominant method for propagation modeling for site-specific scenarios. These techniques can make full use of site-specific building databases, and hence allow for the position of individual buildings to be considered in detail and thus provide site-specific complex channel impulse response information. Also, due to the fact that ray tracing produces deterministic channel models by processing user-defined environments (databases), the analysis can be repeated easily for a variety of different environments.

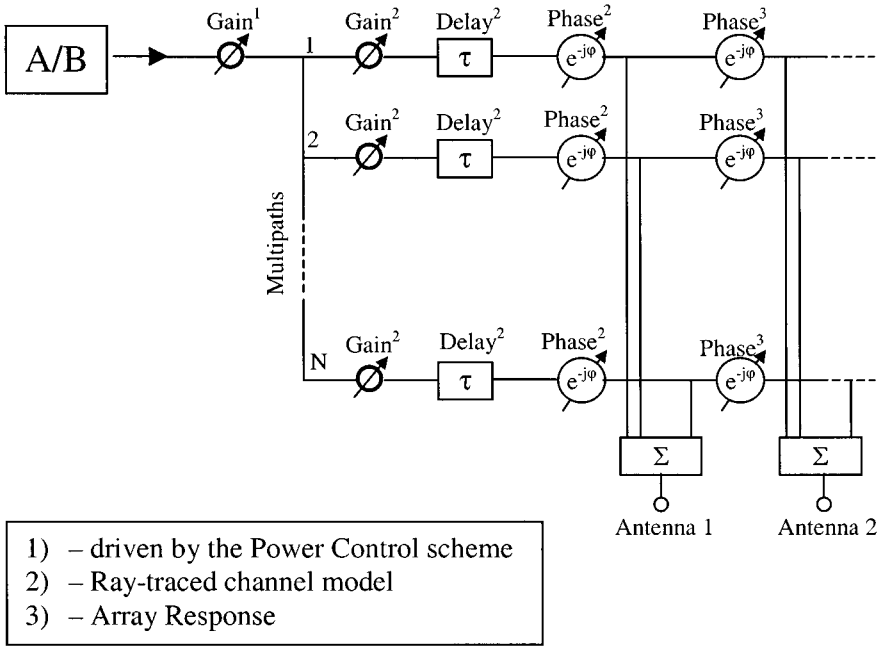

Fig. 4. Radio channel model—a bank of tapped delay lines.

The model employed in the analyses performed in this paper allows for the rapid generation of complex channel impulse response characteristics, and, with sufficient memory, can evaluate scenarios incorporating many thousands of objects. It evolved as the 3-D extension of the ray-tracing algorithm presented in [21]–[23], but now all building databases, illumination zones, and blocking algorithms are fully 3-D, while the terrain morphology and the foliage attenuation are also considered. The antennas can now be placed both below and above the surrounding building clutter, and rays can travel above the buildings or be reflected and/or diffracted by the walls. All reflections and diffractions are computed using 3-D vector mathematics. Each wall is characterized by its permittivity, conductivity, and thickness, and the reflection and diffraction coefficients are evaluated as a function of incident angle for a range of different wall materials. The micro model also employs many acceleration techniques based on a spatially structured building database [20].

Raster terrain databases (with 10- or 50-m resolution) are used to calculate the terrain profile along each ray and check for possible blockage. Hence, the usual assumption of the micro models for flat terrain does not hold for this algorithm. Currently, the model supports ground diffractions and reflections, as well as roof top diffractions, only on the vertical plane between the base station (BS) and mobile antennas. The macro model deals with all other scattering from the ground, as well as off-axis rooftop diffraction. The micro algorithm also uses the vector foliage databases to calculate the foliage attenuation for each individual ray, in the same way as the macro model.

The main characteristics of the microcellular propagation model can be summarized as follows:

1) supports small and medium size cells (it has been used for areas up to 2 km by 2 km);
2) employs 3-D vector building databases;
3) supports BS antennas both below and above building heights;
4) uses 3-D vector tree databases to calculate the foliage attenuation on each ray separately;
5) employs raster terrain databases and checks all rays for terrain blockage;
6) incorporates 3-D antenna patterns;
7) supports different antenna polarizations;
8) simulates 3-D corner diffractions and multiple wall reflections;
9) simulates roof top and ground diffractions between the BS and mobile station (MS) antennas;
10) calculates the electric field of each ray using vector mathematics;
11) provides information for the power, time, and 3-D angles of arrival at both the BS and MS antennas for all multipath rays.

The analysis was performed for a 2 km by 2 km area around the University of Bristol, with the base station placed on top of the Queen's Building (87 m above sea level), as shown in Fig. 5(a). Fig. 5(b) displays the 3-D building and foliage vector databases and the raster terrain database employed by the propagation model. The resolution of the analysis was 5 m. The operating frequency was 1800 MHz. Approximately 2000 grid points employed in the simulations. In order to remove multipath rays with very low power, which have no significant effect in the performance of a system, 10- and 30-dB power windows from the strongest ray are employed for the impulse responses. The analysis is performed within a 120° sector for compatibility with the trisectored approach used by most of the current systems.

C. The Smart Antenna Methods

In the following sections, each of the algorithms employed in the simulations is briefly described.

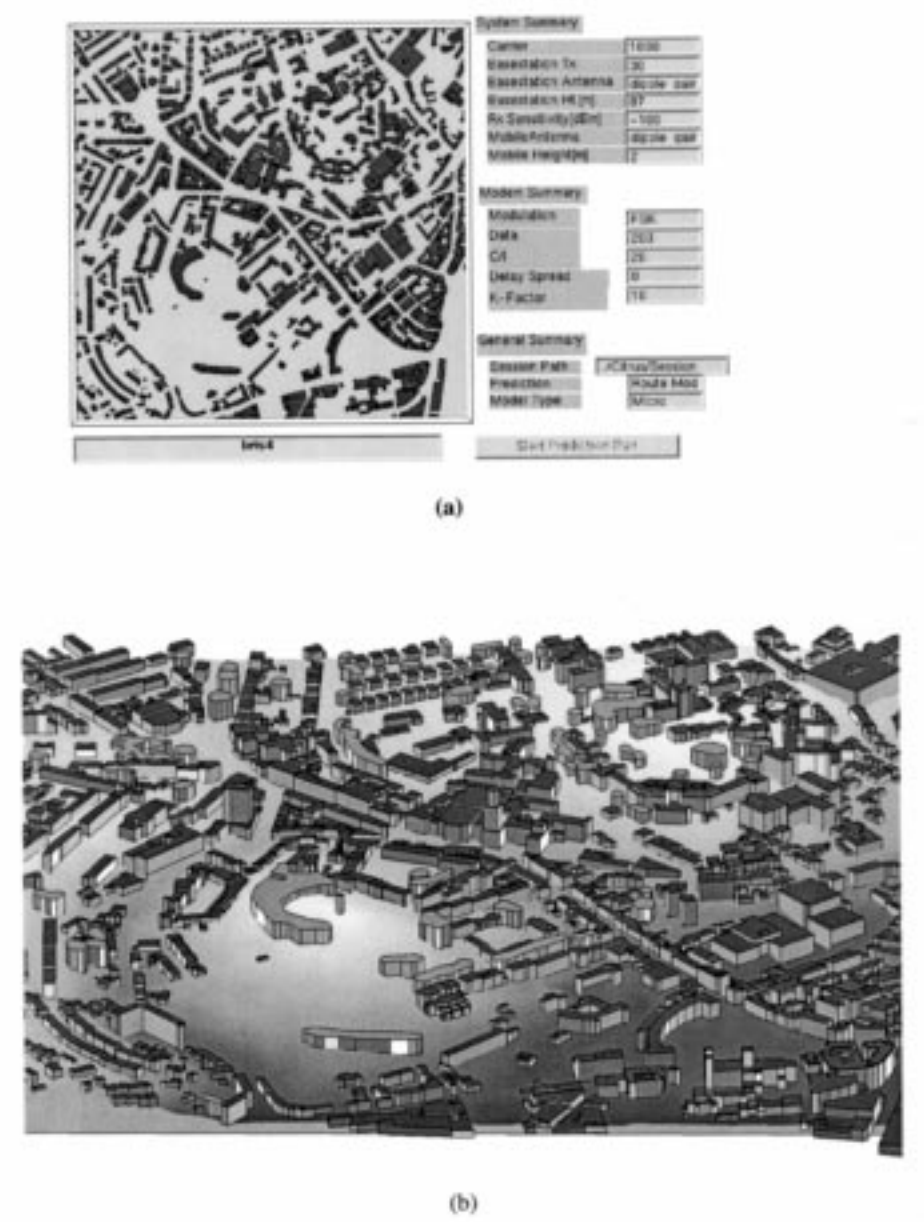

Fig. 5. The (a) two-dimensional and (b) three-dimensional building and foliage vector databases and the raster terrain database employed by the propagation model.

1) Conventional Beamforming–Fourier Method (FM): This classic method is based on the fact that the spatial Fourier transform of an observed signal vector across an array defines the spatial spectrum. The resulting antenna weights can be expressed as

$$w_n = \exp\left(j(n-1)\frac{2\pi}{\lambda}\, d\sin(\varphi)\right) \tag{5}$$

where

φ angle of arrival of the signal;
d interelement distance (0.5λ throughout this paper);
λ wavelength.

It is a straightforward technique, and since it is fairly insensitive to parameter variations, it is inherently robust. In the presence of wide signal separations, this method may offer more robust performance than the high-resolution methods, and since it is far easier to compute, it is a favored candidate in real system implementations.

2) Switched Beams (SB): This method uses a number of fixed steered beams, calculates the power level at the output of each of the beams, and in its simplest form the beam with the highest output power is selected for reception. Although it is believed that this algorithm is best suited to environments in which the received signal has a well —defined direction of arrival, i.e., the angular spread of the environment should be less than the beamwidth of each of the beams, even in environments where the angular spreading is high, there can be benefit from this algorithm. It is not efficient when cochannel interference is present, but it may cope with frequency-selective channels provided the channel consists of narrow clusters at widely separated directions of arrival. This algorithm could

also be used to generate an initial guess at the optimum weight vector for a more sophisticated tracking algorithm.

Two different cases were considered in the simulations:

1) 13 beams spaced at 10° intervals within a 120° sector, (SB13);
2) nine beams spaced at 15° intervals (SB9).

The corresponding beampatterns can be calculated as

$$f(\varphi') = \sum_{n=1}^{N} w_n^* e^{j(n-1)\pi \sin(\varphi')} \tag{6}$$

where φ' ranges within the 120° sector and w_n can be calculated, e.g., using (5) with φ the main beam direction of each beam. Then the ith beam, which gives the maximum output power, is chosen

$$\boldsymbol{P}_{\mathrm{SB}} = \boldsymbol{w}_i^H \boldsymbol{R} \boldsymbol{w}_i, \quad i \in [1, \ldots, 13] \quad \text{or} \quad i \in [1, \ldots, 9] \tag{7}$$

$$P_i = \max(\boldsymbol{P}_{SB}). \tag{8}$$

For both of the above cases, a linear array with eight elements was used. The weights that generate the beams for the SB methods (as for the weights of all the algorithms that are employed in the simulation results shown here) are normalized to the absolute value of the weight vector. In an attempt to balance the conflicting requirements not to consider ideal situations (<-60 dB) and at the same time not to bias the analysis at this level with high sidelobe and null depth levels (>-15 dB), the minimum null depth was chosen to be limited to -30 dB.

The complexity associated with adaptively scanning the beam-pointing direction by varying complex weights in a beamforming network is avoided by switching between fixed beam directions. The weights that produce the desired grid of beams can be calculated and saved for future use; hence the beam switching approach allows the multibeam antenna and switch matrix to be easily integrated with existing cell site receivers as an applique [14]. Also, tracking is performed at beam switching rate (compared to angular change rate for direction finding methods and fading change rate for optimum combining [2]). Disadvantages include low gain between beams, limited interference suppression and false locking with shadowing, interference, and wide angular spread [2].

3) Combined Switched Beam Approach (SBc): The difference between this method and the basic switched beam approach is that in this case, the calculated power levels at the output of each of the beams are considered in the context of a power window threshold (from the maximum power), and all the beams with output power within the employed power window are selected. The default power windows were chosen to be 3 and 5 dB for SB13 and SB9, respectively. These default values were chosen 1) bearing in mind the measurements reported in [14] and also in an attempt to balance the different beam spacing between the two methods as well as the conflicting requirements of capturing as much desired energy as possible and avoiding interference. As a result, two different cases are considered: SB13c and SB9c.

Combining the best beams from a grid of beams is slightly more complex than the basic grid of beams approach. It requires processing the outputs from all the beams in order to find which beams give power within the chosen power window, and then summation of the chosen output signals.

4) Beam Space Optimum Combining (BOPC): This method works with the eigenvalues of the calculated correlation matrix. The eigenvalues of a correlation matrix indicate how dispersive (spatially) the received signal is. If there are a few eigenvalues with similar amplitudes, then the variability of the signal will tend to be confined to the subspace spanned by the corresponding eigendirections. If the eigenvalues are approximately equal, then the signal spans the full multidimensional space. If a power window is employed for the eigenvalues of the correlation matrix, then a mechanism is automatically generated to control how many degrees of freedom will be used. The chosen power window can be fixed to some predefined value, or can be adaptive to each scenario considered. After the calculation of eigenvalues, the corresponding eigenvectors of the covariance matrix are simply combined in an optimum manner.

From [24], for the eigenvalue solution in array space for maximum signal-to-(interference plus noise) ratio (SINR) at the output of a smart antenna

$$\boldsymbol{w}_{\mathrm{opt}} = \boldsymbol{R}_{xx}^{-1} \boldsymbol{v}_{\max} \tag{9}$$

where $\boldsymbol{v}_{\max}$ is the associated eigenvector to the largest eigenvalue $\lambda_{\max}$ of $\boldsymbol{R}_{xx}$. It was shown in [12] that the eigenvector that corresponds to the maximum eigenvalue of the correlation matrix is approximately equal to the steering vector of the target signal source (desired signal) when the desired signal is much stronger than the interferers at the receiver. As a result, this technique is particularly applicable to CDMA systems due to the available processing gain. This technique is suboptimal in that it does not null out interference. Although it is rather complex $(O(3\ \mathrm{N}^2 + 12\ \mathrm{N}))$, it is very promising since there have been ways suggested in [12] to reduce its complexity down to $O(11\ \mathrm{N})$.

D. Processing of the Results

The users in the simulations are chosen randomly with the only criterion being their position. In this context, and employing a Monte Carlo approach, the above steps of the analysis are repeated many times (typically 1000) for different positions of users. With this method, the statistics [probability distribution function (pdf) and cumulative distribution function (cdf)] of the SINR gain achieved with the smart antenna methods can be calculated, and hence, more secure and reliable performance results can be estimated.

III. Simulation Results

A. Low Bit Rate Desired and Interfering Users

Fig. 6 shows results for the case of low bit rate desired and interfering users. The pdfs of the achieved gain with the different algorithms and 50 interfering users are shown in Fig. 6(a), while Fig. 6(b) shows the cdf of these gains. Other traditional algorithms like temporal reference beamforming (OPC), minimum variance distortionless response (MVDR), and maximum entropy method (MEM) are also shown for reference (calculation of the weights for these algorithms was based on [3] and

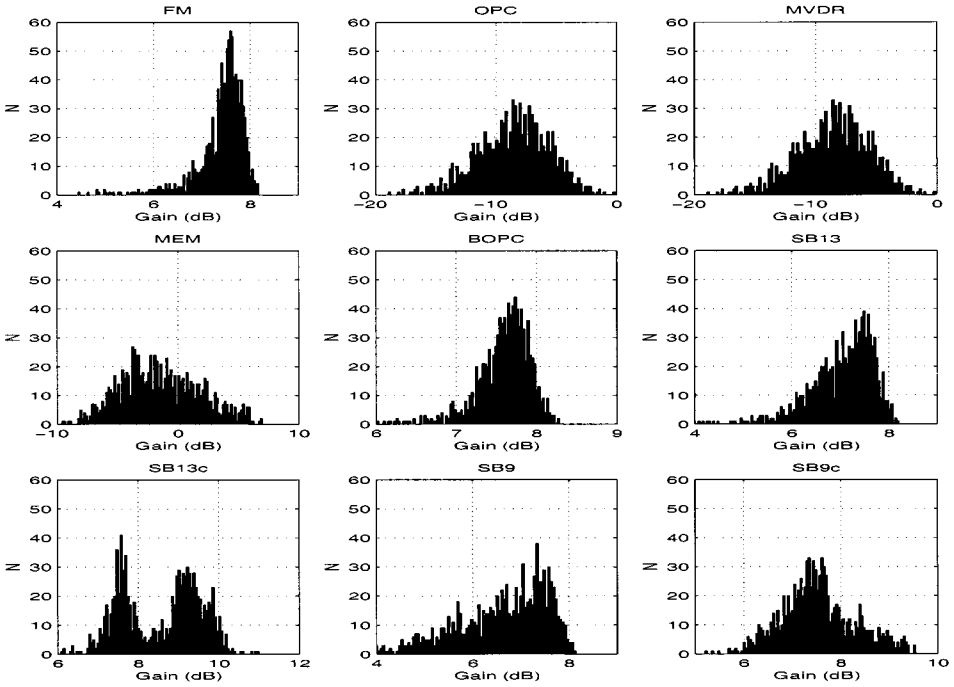

(a)

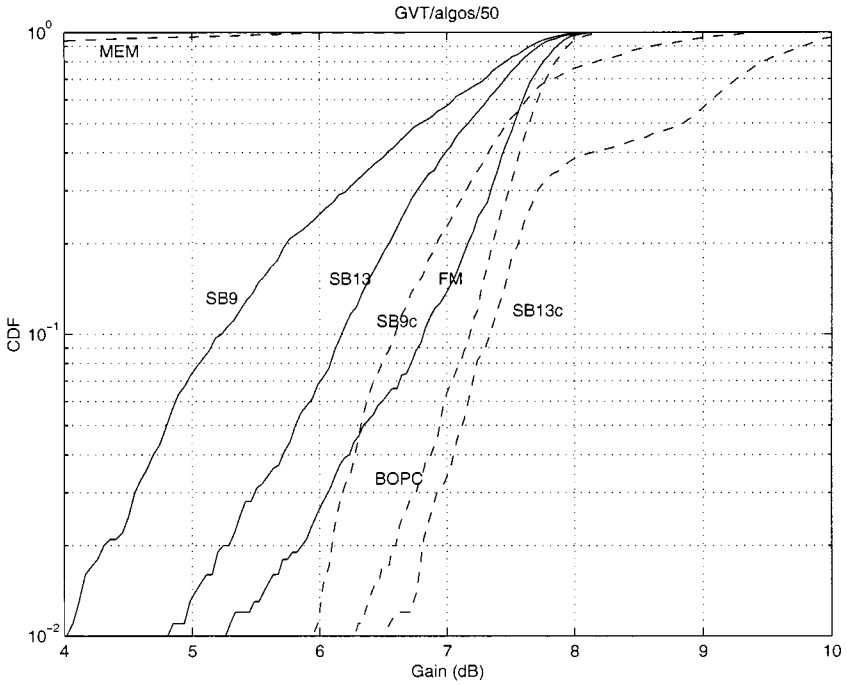

(b)

Fig. 6. Output gain (dB) for the different algorithms with 51 LBR users: (a) pdfs and (b) cdfs.

[4]). All of these three algorithms have difficulties with the scenarios studied here, as can be seen from the second, third, and fourth graphs of Fig. 6(a). The basic problem for temporal reference-based beamforming algorithms for FRAMES mode-2 W-CDMA is the uplink frame structure. The "IQ data/control" channel multiplexing, although beneficial for electromagnetic compatibility (avoids discontinuous transmission), inserts pilot bits only into one control branch. When the pilot is used as a time reference signal for the optimum combining schemes, the other branch (data) is seen as an interfering signal with the same space–time characteristics. This leads to performance degradation, since the desired signal is partially cancelled. Ways to

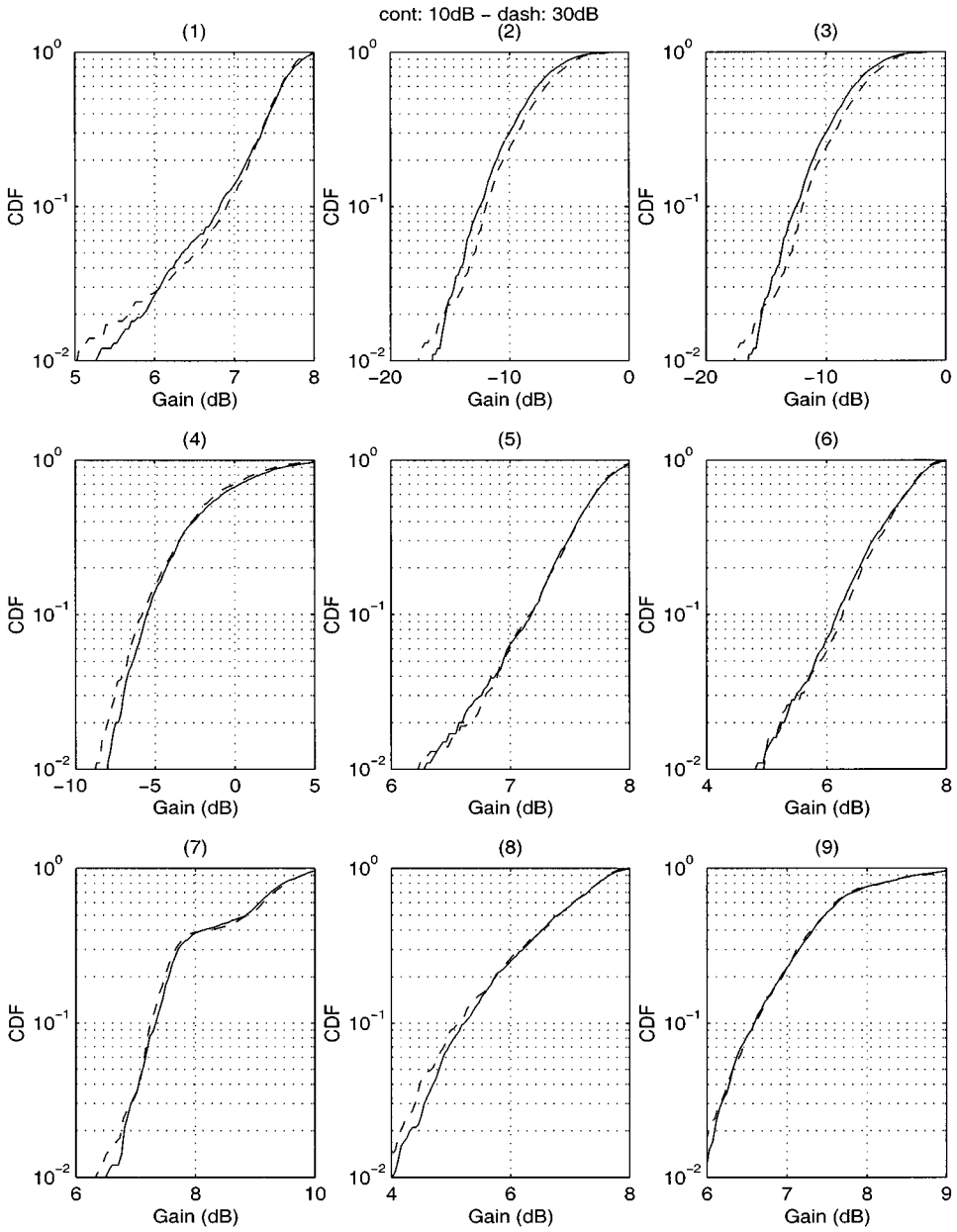

Fig. 7. Output gain (dB) for the different algorithms with 51 LBR users with 10- and 30-dB power window for the impulse responses. (1) FM, (2) OPC, (3) MVDR, (4) MEM, (5) BOPC, (6) SB13, (7) SB13c, (8) SB9, and (9) SB9c.

avoid this situation may be to use blindly recovered data bits as an additional time reference [24], or to use the maximum signal to interference plus noise criterion with totally suppressed desired signal [26].

All the other algorithms manage to achieve positive gains always, up to the 9 dB theoretical maximum gain. The two switched-beam versions that employ combining can obviously exceed this threshold. Fig. 6(b) shows that all the algorithms apart from the OPC-MVDR-MEM can achieve more than 4-dB gains. The combined versions of the switched beams are better than their basic versions, and the version with 13 beams is better than the version with nine beams (with or without combining). With 90% probability, SB13 and SB13c are $\sim$1 dB better than SB9 and SB9c, respectively. Also, it was noticed that there are cases when the combined switched beam versions can achieve much higher gain values. The FM method shows $\sim$0.5 dB worse performance than the BOPC algorithm, which is the best non-combined method[1] and with 90% probability can achieve $\sim$7 dB gain, close to the SB13c method, which has the best overall performance. It is interesting to notice that the FM algorithm outperforms both the SB9 and the SB13, and its performance is generally close to the SB9c method (apart from the region with the high gain values for SB9c). Overall, the FM algorithm seems to be the first choice in terms of balancing performance

[1]This result agrees with the result from [27] that the tracking beam array (BOPC here) is superior to the switching beam array when the desired signal is sufficiently larger than each of the interferers at the receiver.

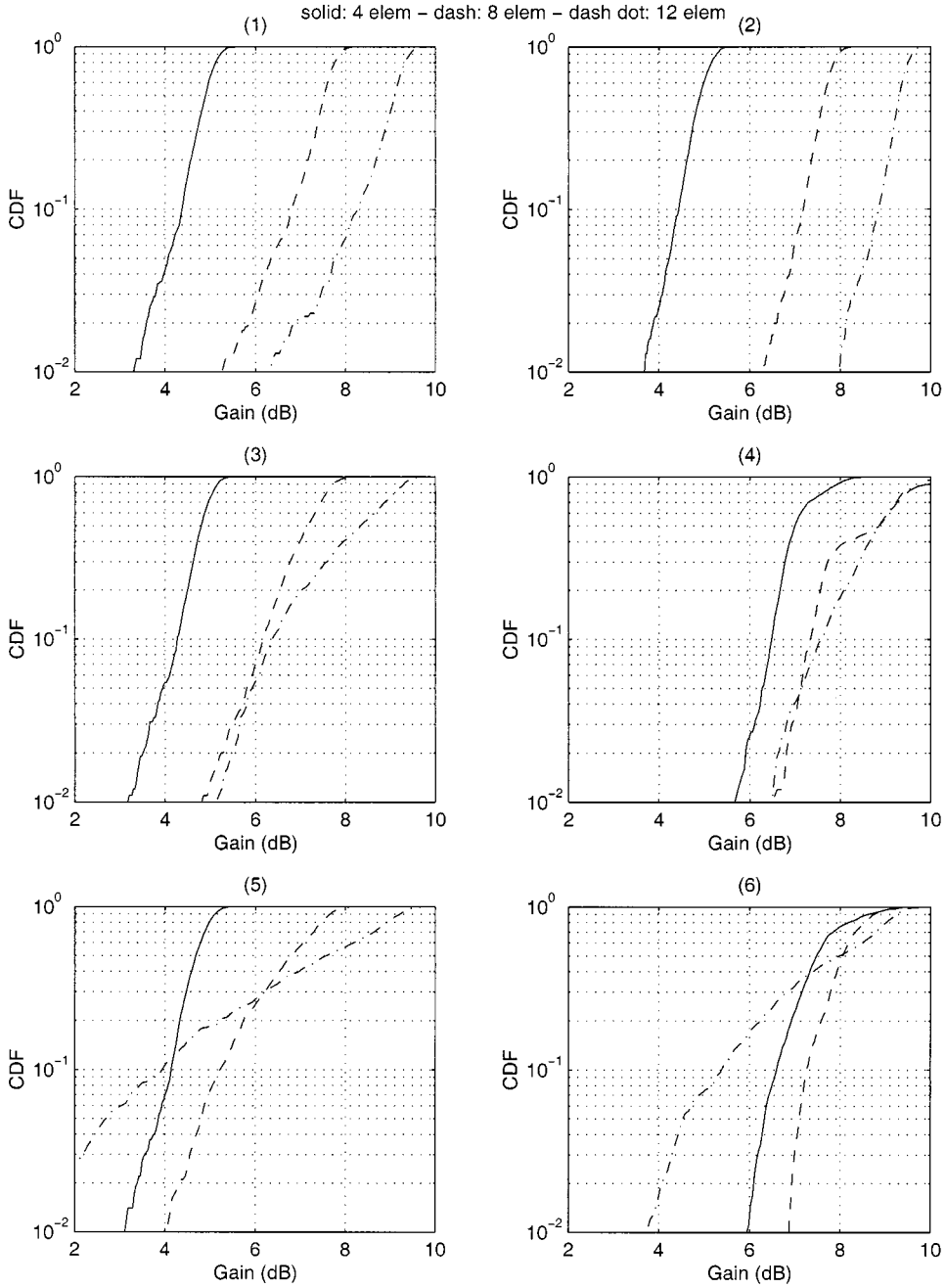

Fig. 8. Output gain (dB) for the different algorithms with 51 LBR users as a function of the number of array elements. (1) FM, (2) BOPC, (3) SB13, (4) SB13c, (5) SB9, and (6) SB9c.

and complexity, with the next option the combined version of switched beam method with 13 beams and BOPC.

B. Sensitivity of the Performance to Environmental and System Parameters

In order to investigate the sensitivity of the performance of the employed algorithms, three cases are considered. First, the performance when the impulse responses used in the simulations employ 10- and 30-dB windows (i.e., sensitivity to the environment) (Fig. 7), the performance with different number of array elements (Fig. 8), and finally the performance as a function of the accuracy of the amplitude and phase of the calculated weights (Fig. 9). In terms of the performance with respect to the level of interference from other than the central cell, it was noticed that since the algorithms do not attempt directly to reduce interference but to capture the desired signal, seem to be robust against other cell interference (less than 0.5 dB change for levels from 5 to 15 dB below the total central cell interference).

Fig. 7 shows that the performance difference between the case of impulse responses with 10- and 30-dB power windows is small for the OPC-MVDR-MEM algorithms and negligible for all the others. For the algorithms that manage to produce positive gains, this implies that they are robust against relatively low-power multipaths.

Fig. 8 shows results for the cases with four, eight, and 12 array elements. For the cases of the FM and BOPC algorithms, more elements result in better output gain, with better improvement for the increase from four to eight elements. For the SB13 case, increasing the number of elements from four to eight offers an additional $\sim$2 dB gain, while a further increase to 12 elements seems to have little effect. The reason is that although the beams are more narrow with 12 elements, they cross at $\sim$4 dB below the peak now (instead of $\sim$3 dB with eight elements). Hence there is a reduction due to the users who fall between two beams. The same holds for the SB9, where it can be seen that an increase from eight to 12 elements would actually decrease, for some cases, the output gain. Similar behavior with the relevant basic versions can be noticed for the two combined switched beam cases.

Fig. 9 shows results for the effect that weight amplitude and phase mismatches have on the performance of the FM, BOPC, SB13, and SB9 algorithms. The method employed here to simulate the weight distortions was the one presented by Weiss and Friedlander in [28]. This involves generating values for the amplitude and phase of each element and then perturbing them from the ideal by a random variable with a specified variance. The cases studied are:

a) ideal;
b) 0.1-dB amplitude variance;
c) 0.5-dB amplitude variance;
d) 10° phase variance;
e) 30° phase variance;
f) 0.5-dB amplitude and 30° phase variance

Fig. 9(a) shows that amplitude and phase mismatches lead to distortions of the produced radiation pattern and hence reduced output gain [values from left to right at the titles of each subplot correspond to the cases (a)–(f)]. Reductions up to $\sim$4 dB in the output gain can be seen from Fig. 9(b). From the same figure can be seen that 0.1-dB amplitude and less than 10° phase distortion will be required for the produced weights of all the algorithms in order to avoid performance degradation.

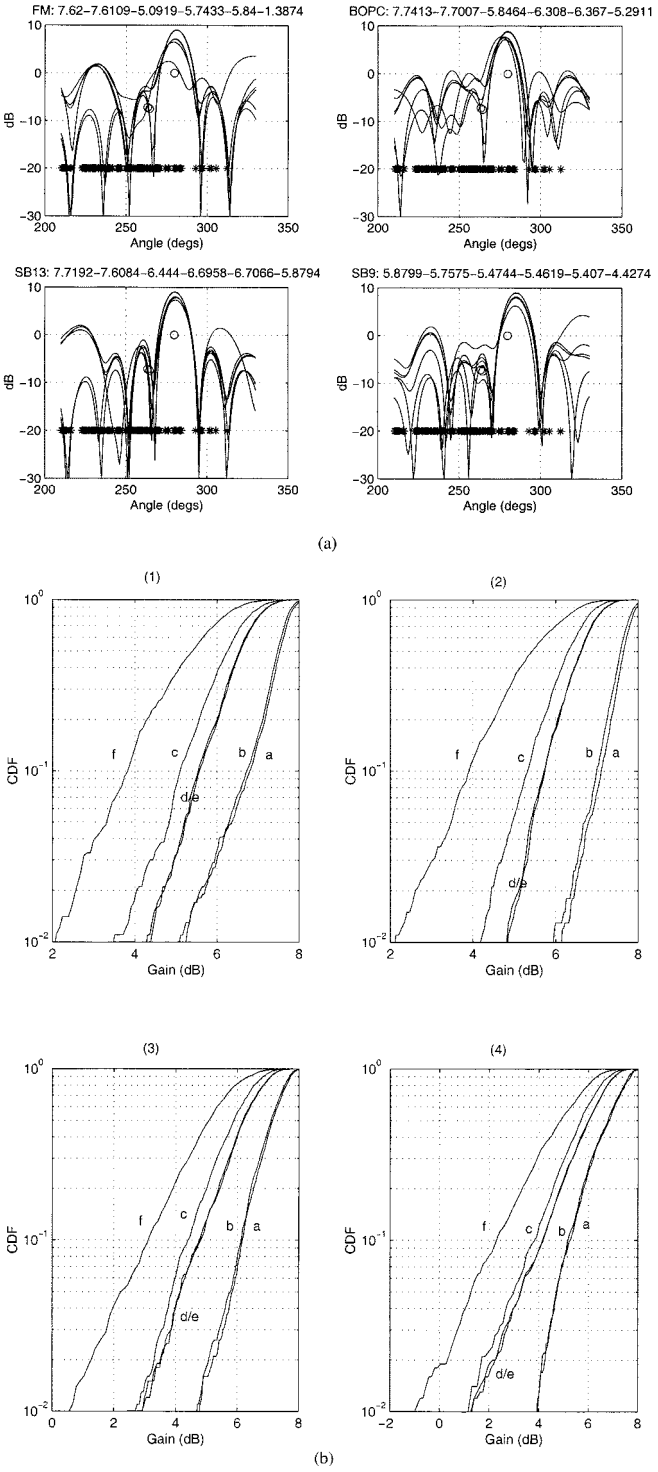

Fig. 9. Sensitivity of the (1) FM, (2) BOPC, (3) SB13, and (4) SB9 methods to the amplitude and phase accuracy of the calculated weights: (a) radiation pattern examples and (b) cdfs of the output gain.

C. Different System Loading (LBR Users)

Fig. 10 shows the cdfs for each algorithm with 50 to 200 LBR interfering users. As was expected, since the more the central cell is loaded the higher the probability to receive interference from the main lobe (or lobes in the cases of the combined switched beams and the BOPC) of the radiation pattern is, smaller output gain values are noticed. For all the algorithms, the gain reduction in all cases is less than $\sim$2 dB, with 90% probability.

D. Low- and High-Bit-Rate User Scenarios

Fig. 11 shows results for the cdfs of the output gain for the cases of 51 (one desired and 50 interfering) LBR users and 46 (one desired and 45 interfering) LBR users and five high-bit-rate (HBR) users (spreading factor SF $= 8$). It can be seen that in all cases apart from the two combined switched-beam approaches, there is a reduction in the output gain $\sim$2 dB (90% probability). This can be attributed to the increased level of interference from the HBR users (lack of spreading gain). In this case, the desired signal is not much stronger than the interferers at the receiver, and as a result, the eigenvector that corresponds to the maximum eigenvalue of the correlation matrix will deviate from the true value of the steering vector of the target signal source, which ultimately leads to performance degradation (in agreement with the conclusions from [27]).

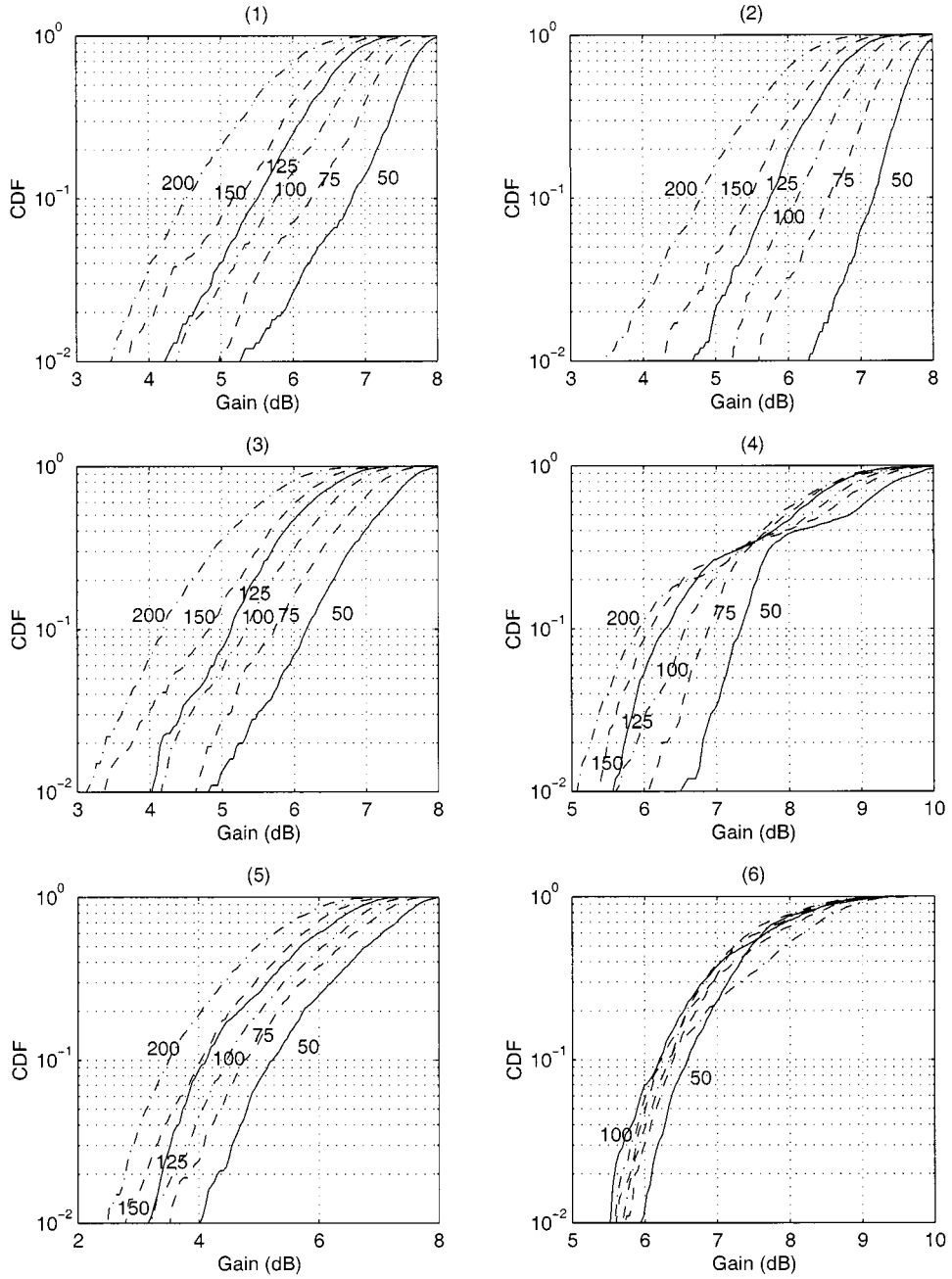

Fig. 10. Output gain (dB) with 50 to 200 LBR users. (1) FM, (2) BOPC, (3) SB13, (4) SB13c, (5) SB9, and (6) SB9c.

The reduction for SB13c is somewhat smaller ($\sim$1 dB) for 90% probability, but it is interesting to see that with low probability, the output gains are similar to the case of 51 LBR users. This behavior is more evident for the SB9c method, where the output gain is better for the HBR users than the LBR case. This result indicates a possible problem with the combined switched beam approaches for the case of HBR users. In such a scenario, the algorithm might perceive the energy from the HBR interfering users as desired energy, use additional beams in order to capture it, and hence produce an erroneous output.

In order to study further this situation, the results shown in Fig. 12 were produced, where different combinations of desired and interfering user spreading factors (bit rates) were considered. The different lines in Fig. 12 correspond to the following cases (DU: desired user; IU: interfering users;, SF: spreading factor):

a) solid dot: DUSF $= 256$; 50 IUSF $= 256$;
b) solid: DUSF $= 32$; 50 IUSF $= 256$;
c) dash: DUSF $= 32$, 45 IUSF $= 256$; 5 IUSF $= 64$;
d) dash-dot: DUSF $= 32$; 45 IUSF $= 256$; 5 IUSF $= 32$;
e) dot: DUSF $= 32$; 45 IUSF $= 8$.

Several things can be noticed from Fig. 12. First, the higher the bit rate of the desired user, the more the output gain; see cases a) and b). Then, the higher the bit rate for the interferers, the more the output gain is reduced. Nevertheless, this reduction is quite small (less than 0.5 dB), and it affects less the switched beam approaches [cases b)–d)]. Furthermore, this holds as long

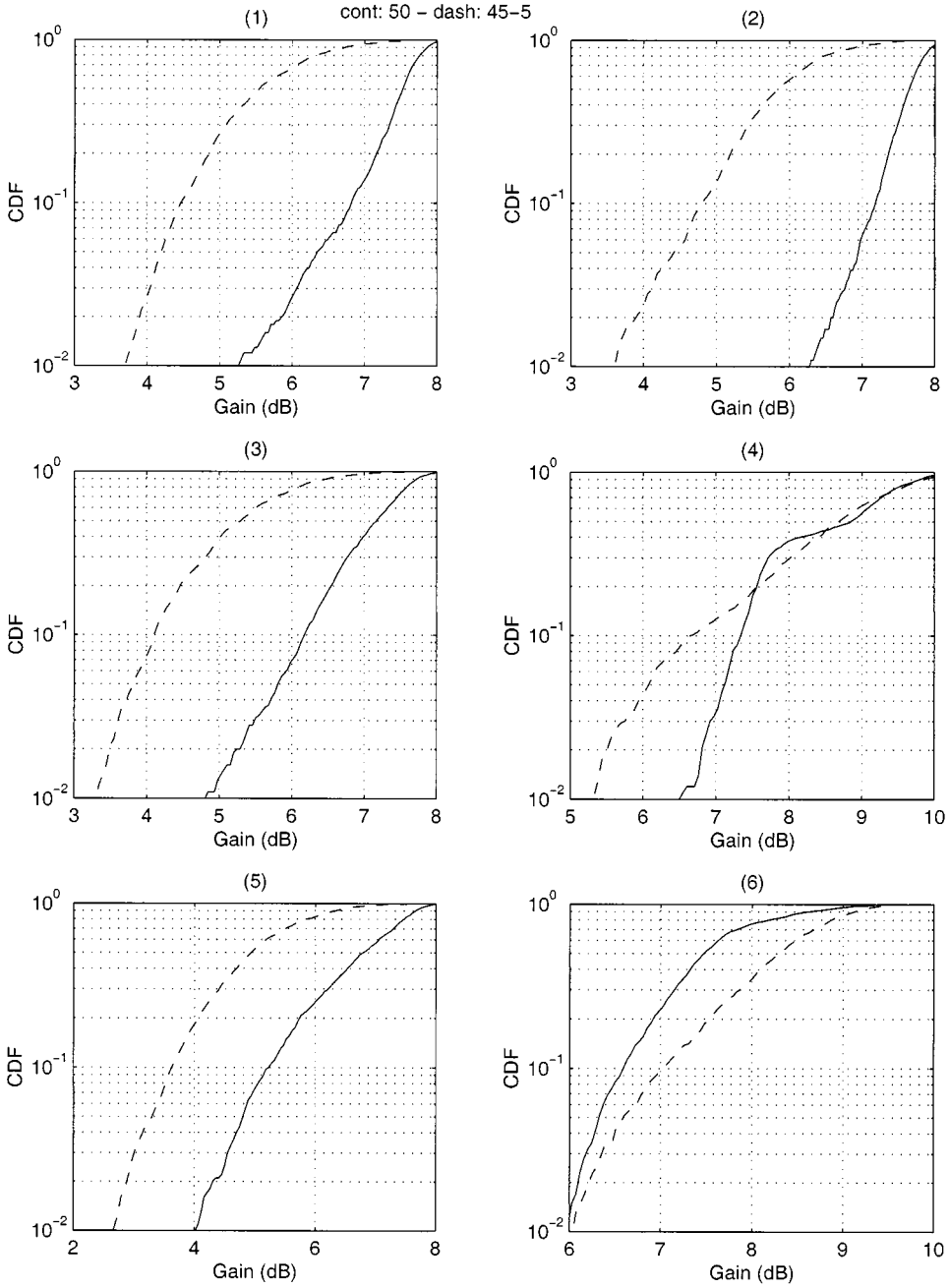

Fig. 11. Output gain (dB) for the different algorithms with 45 interfering plus the desired LBR users and five interfering HBR users (SF = 8). (1) FM, (2) BOPC, (3) SB13, (4) SB13c, (5) SB9, and (6) SB9c.

as there are no very HBR interfering users [case e)]. In this case, the gain is reduced more (1.5–2 dB for FM-BOPC and ∼1 dB for the rest of the algorithms; −90% probability).

IV. Conclusions

For the typical scenario of a system with 51 low-bit-rate users, the combined versions of the switched beams are better than their basic versions, and the version with 13 beams is better than that with nine beams (with or without combining). With 90% probability, SB13 and SB13c are ∼1 dB better than SB9 and SB9c, respectively. The FM method shows ∼0.5 dB worse performance than the BOPC algorithm, which is the best non-combined method and with 90% probability can achieve ∼7 dB gain, close to the SB13c method, which has the best overall performance. The FM algorithm outperforms both the SB9 and the SB13, and its performance is generally close to the SB9c method. The analysis showed that although the fixed beam approaches can give acceptable gains, the adaptive steering of the main beam to the direction of maximum energy is better. Selection of more than one beam (within a given power window) and subsequent combining can produce better gain, but one should be careful in balancing the conflicting requirements of desired energy capturing and interference reduction. In terms of the sensitivity of these algorithms to several parameters, the following were seen.

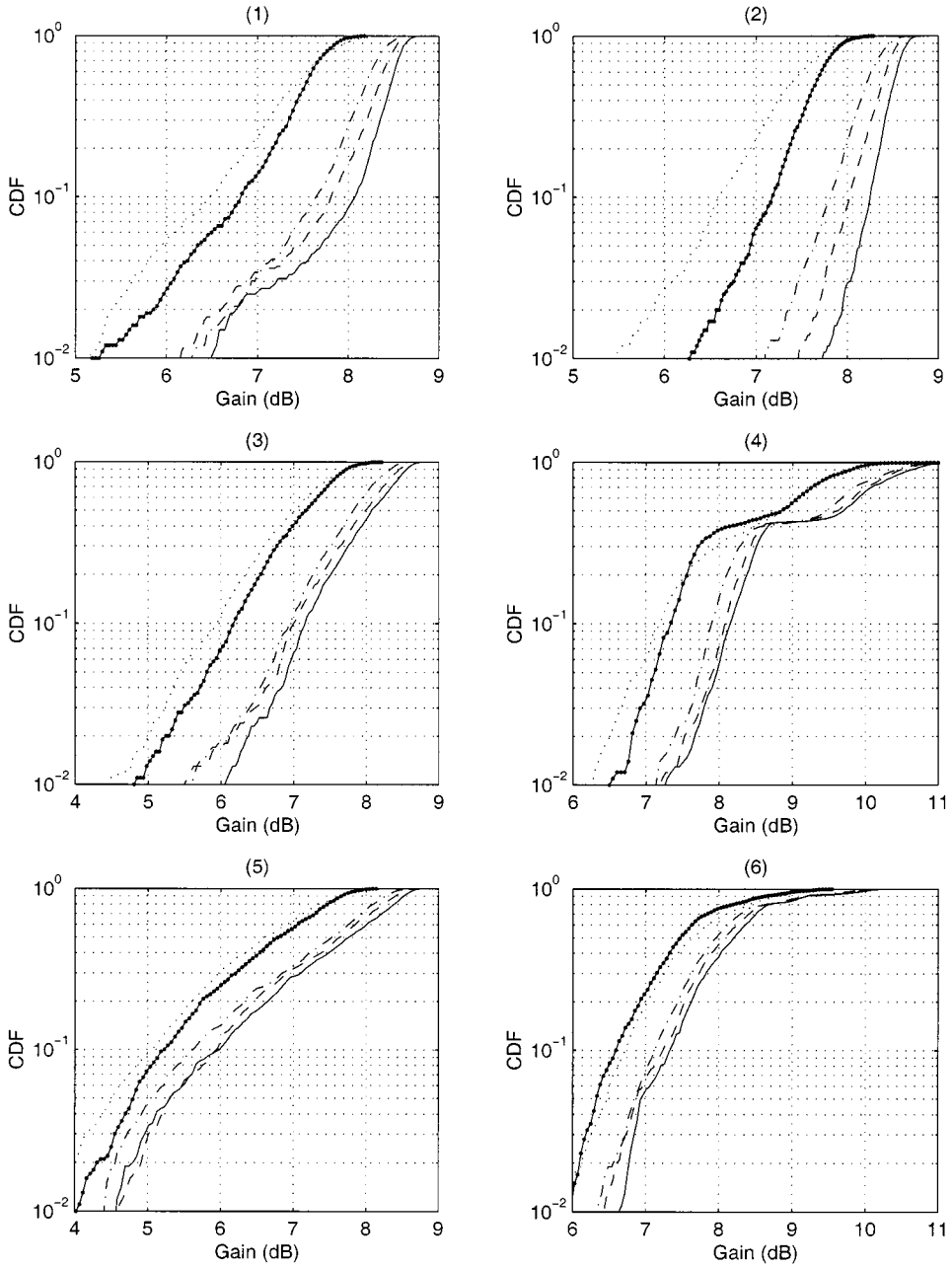

Fig. 12. Output gain with 50 users and different spreading factor combinations. (1) FM, (2) BOPC, (3) SB13, (4) SB13c, (5) SB9, and (6) SB9c.

1) The performance difference between the case of impulse responses with 10- and 30-dB power windows is negligible, which implies that they are robust against relatively low power multipaths.
2) For the cases of the FM and BOPC algorithms, more elements result in better output gain, with better improvement for the increase from four to eight elements. For the SB13 case, increasing the number of elements from four to eight offers an additional $\sim$2 dB gain, while a further increase to 12 elements seems to have little effect. Similar behavior was noticed for the rest of the switched-beam cases. The beamwidth but also the beam crossing level (spacing) are the important parameters for the switched beam methods. Both of these parameters are related to the switching time, the required hysterisis levels, the output gain, and the type of environment in which the multibeam antenna is employed.
3) Amplitude and phase mismatches lead to distortions of the produced radiation pattern and hence reduced output gain. Up to 0.1 dB amplitude and less than 10° phase distortion will be required for the produced weights of all the algorithms examined in this paper in order to avoid performance degradation.

From the different combinations of desired and interfering user bit rates that were considered, several important things were noticed: First, the higher the bit rate of the desired user, the more the output gain. Also, the higher the bit rate for the interferers, the more the output gain is reduced. Nevertheless,

this reduction is quite small (less than 0.5 dB) and affects the switched-beam approaches less. Furthermore, this holds as long as there are no very HBR interfering users. In this case, the gain is reduced more (1.5–2 dB for the FM-BOPC and $\sim$1 dB for the rest of the algorithms—90% probability). Finally, for scenarios with HBR interfering users, all the algorithms apart from the FM might perceive the energy from the HBR interfering users as desired energy, attempt to capture it, and hence produce an erroneous output.

Overall, the conventional beamforming algorithm seems to be the first choice in terms of balancing performance and complexity, in particular when the problem with interfering HBR W-CDMA users is considered. Close to the FM method but with lower overall performance comes the switched-beam method with 13 beams.

ACKNOWLEDGMENT

The authors wish to thank Prof. J. McGeehan, Dr. M. Beach, and Dr. A. Nix for their support during this activity. R. Piechocki wishes to thank Fujitsu Europe Telecom R & D Centre, Ltd. for sponsoring his Ph. D. work.

REFERENCES

[1] J. Rapeli, "UMTS: Targets, system concept, and standardization in a global framework," *IEEE Personal Commun.*, vol. 2, pp. 20–28, Feb. 1995.

[2] G. V. Tsoulos, "Smart antennas for mobile communications systems: Benefits and challenges," *Electron. Commun. Eng. J.*, vol. 11, no. 2, pp. 84–94, Apr. 1999.

[3] L. Godara, "Applications of antenna arrays to mobile communications, Part II: Beamforming and direction-of-arrival considerations," *Proc. IEEE*, vol. 85, pp. 1195–1245, Aug. 1997.

[4] S. Haykin, J. Reilly, V. Kezys, and E. Vertatschitsch, "Some aspects of array signal processing," *Proc. Inst. Elect. Eng. F*, vol. 139, no. 1, pp. 1–26, Feb. 1992.

[5] S. C. Swales, M. A. Beach, and J. P. McGeehan, "The performance enhancement of multi-beam adaptive base station antennas for cellular land mobile radio systems," *IEEE Trans. Veh. Technol.*, vol. 39, pp. 56–67, Feb. 1990.

[6] R. Kohno, H. Imai, M. Hatori, and S. Pasupathy, "Combination of an adaptive array antenna and a canceller of interference for direct sequence spread spectrum multiple access system," *IEEE J. Select. Areas Commun.*, vol. 8, pp. 675–682, May 1990.

[7] J. H. Winters, "Upper bounds on the BER of optimum combining," in *Proc. IEEE 44th Vehicular Technology Conf.*, vol. 2, Stockholm, Sweden, June 8–10, 1994, pp. 942–946.

[8] A. Naguib, A. Paulraj, and T. Kailath, "Capacity improvement with base station antenna arrays in cellular CDMA," *IEEE Trans. Veh. Technol.*, vol. 43, pp. 691–698, Aug. 1994.

[9] G. V. Tsoulos, M. A. Beach, and S. C. Swales, "Adaptive antennas for third generation DS-CDMA cellular systems," in *Proc. 45th Vehicular Technology Conf.*, vol. 1, Chicago, IL, July 1995, pp. 45–49.

[10] P. Zetterberg and B. Ottersten, "The spectrum efficiency of base station antenna array system for spatially selective transmission," *IEEE Trans. Veh. Technol.*, vol. 44, pp. 651–660, Aug. 1995.

[11] J. Thompson, P. Grant, and B. Mulgrew, "Smart antenna arrays for CDMA systems," *IEEE Personal Commun.*, vol. 3, pp. 16–25, Oct. 1996.

[12] S. Choi and D. Yun, "Design of an adaptive antenna array for tracking the source of maximum power and its application to CDMA mobile communications," *IEEE Trans. Antennas Propagat.*, vol. 45, pp. 1393–1404, Sept. 1997.

[13] Y. Ogawa, Y. Nagashima, and K. Itoh, "An adaptive antenna system for high speed digital mobile communications," *IEEE Trans. Commun.*, pp. 413–421, May 1992.

[14] Y. Li, M. Feuerstein, and D. Reudink, "Performance evaluation of a cellular base station multi beam antenna," *IEEE Trans. Veh. Technol.*, vol. 46, pp. 1–9, 1997.

[15] G. V. Tsoulos, J. McGeehan, and M. Beach, "Space division multiple access (SDMA) field trials—Part I: Tracking and BER performance," in *Proc. Inst. Elect. Eng. Radar, Sonar Navigat. (Special Issue on Antenna Array Processing Techniques)*, Feb. 1998, pp. 73–78.

[16] ——, "Space division multiple access (SDMA) field trials—Part II: Calibration and linearity issues," in *Proc. Inst. Elect. Eng. Radar, Sonar Navigat. (Special Issue on Antenna Array Processing Techniques)*, Feb. 1998, pp. 79–84.

[17] A. Paulraj and C. Papadias, "Space-Time processing for wireless communications," *IEEE Signal Processing Mag.*, pp. 49–83, Nov. 1997.

[18] European Telecommunications Standards Institute, , " ETSI UMTS terrestrial radio access (UTRA) ITU-R RTT candidate submission,", 1998.

[19] R. Piechocki, "Multi-rate wideband DS-CDMA architectures with adaptive antennas for third generation mobile communications," Univ. of Bristol, Ph.D. Transfer Rep., Oct. 1998.

[20] G. E. Athanasiadou, E. K. Tameh, and A. R. Nix, "Channel impulse three-dimensional rural-urban simulator (CITRUS): An integrated micro-macro ray-based propagation model which employs raster and vector building databases simultaneously," in *Proc. IEEE PIMRC'99*, Osaka, Japan, Sept. 1999.

[21] G. E. Athanasiadou, A. R. Nix, and J. P. McGeehan, "A ray tracing algorithm for microcellular wideband propagation modeling," in *Proc. IEEE VTC '95*, Chicago, IL, July 25–28, 1995, pp. 261–265.

[22] ——, "Comparison of predictions from a ray tracing microcellular model with narrowband measurements," in *Proc. IEEE VTC '97*, Phoenix, AZ, May 4–7, 1997, pp. 800–804.

[23] ——, "A microcellular ray-tracing propagation model and evaluation of its narrowband and wideband predictions," IEEE J. Select. Areas Commun., vol. 48, 1999, to be published.

[24] J. E. Hudson, *Adaptive Array Principles*: Peter Peregrinus Ltd., 1981.

[25] X. Mestre, J. Fonollosa, and G. Vazques, "Uplink beamforming for the FDD mode of UTRA," in *Vehicular Technology Conference—VTC'99*, Houston, TX, May 1999.

[26] R. J. Piechocki, N. Canagarajah, J. P. McGeehan, and G. V. Tsoulos, "Orthogonal re-spread for uplink W-CDMA beamforming," in *VTC2000-Spring*, Tokyo, Japan, May 15–18, 2000.

[27] S. Choi, D. Shim, and T. Sarkar, "A comparison of tracking beam arrays and switching beam arrays operating in a CDMA mobile communication channel," *IEEE Antennas Propagat. Mag.*, vol. 41, pp. 10–22, Dec. 1999.

[28] A. Weis and B. Friedlander, "Directional finding in the presence of mutual coupling," in *Proc. 22nd Asilomar Conf. Signals, Systems and Computers*, 1988, pp. 598–602.

George V. Tsoulos (M'94) received the Ph.D. degree from the University of Bristol, U.K., in 1996 and the first degree in electrical and computer engineering from the National Technical University of Athens, Greece, in 1992.

While at the Centre for Communications Research of the University of Bristol, he was actively involved in all three pioneering European collaborative research projects on adaptive antennas (RACE TSUNAMI I, ACTS TSUNAMI II, and SUNBEAM). In 1998, he became a Research Fellow at the University of Bristol, where his work focused on the area of smart antenna techniques for third-generation mobile communications. Dr. Tsoulos is the author of more than 50 international publications and more than 20 technical reports on adaptive antenna related topics. He is a Member of the organizing committee of the European action COST 260 on smart antennas and an Expert Member of the COST action 259, the Technical Chamber of Greece. He joined the wireless technology practice of the Technology Centre of the PA Consulting Group, Cambridge, U.K., in 1999. His current interests include design, optimization, and implementation of "intelligent" wireless and broadband communication systems with smart antennas.

Georgia E. Athanasiadou (M'00) received the first degree in electrical and computer engineering from the National Technical University of Athens, Greece, in 1992 and the Ph.D. degree from the University of Bristol, U.K., in 1997.

From October 1996 to October 1999, she was a Research Associate and then a Research Fellow at the Centre for Communications Research, University of Bristol, working in the area of radio propagation modeling. As part of her research, she has developed, investigated, and evaluated novel indoor and outdoor ray-tracing propagation models. Her research interests include network planning issues with ray-tracing models for different air interface techniques, with particular emphasis on adaptive antennas and future generation systems. She is now a Senior Research Engineer with Adaptive Broadband Ltd., Cambridge, U.K., working on broadband wireless systems.

Dr. Athanasiadou is a member of the Technical Chamber of Greece.

Robert Piechocki (S '98) received the M.Sc. degree (with first class honors) in electrical engineering from the Technical University of Wroclaw, Poland, in 1997. Since then he has been pursuing a Ph.D. degree at the Centre for Communications Research, University of Bristol, U.K.

His research interests lie in the areas of statistical signal processing for communications and radio channel modeling for wireless systems. He is currently involved in design and optimization of the smart antenna systems for W-CDMA.